Surface-Induced Ordering Depresses Through-Film Ionic Conductivity in Lamellar Block Copolymer Electrolytes

Jonathan P. Coote,[†] Thomas Kinsey,[†] Dayton P. Street,[‡] S. Michael Kilbey, II,[‡,†] Joshua R. Sangoro,[†] and Gila E. Stein[*,†]

[†]*Department of Chemical and Biomolecular Engineering, University of Tennessee, Knoxville, TN 37996, USA*

[‡]*Department of Chemistry, University of Tennessee, Knoxville, TN 37996, USA*

E-mail: gstein4@utk.edu

Abstract

Lamellar block copolymers based on polymeric ionic liquids (PILs) show promise as electrolytes in electrochemical devices. However, these systems often display structural anisotropy that depresses the through-film ionic conductivity. This work hypothesizes that structural anisotropy is a consequence of surface-induced ordering, where preferential adsorption of one block at the electrode drives a short-range stacking of the lamellae. This point was examined with lamellar diblock copolymers of polystyrene (PS) and poly(1-(2-acryloyloxyethyl)-3-butylimidazolium bis(trifluoromethanesulfonyl)imide) (PIL). The bulk PS-PIL structure was comprised of randomly-oriented lamellar grains. However, in thin PS-PIL films (100-400 nm), the lamellae were stacked normal to the plane of the film, and islands/holes were observed when the as-prepared film thickness was incommensurate with the natural lamellar periodicity. Both of these attributes are well-known consequences of preferential wetting

at surfaces. The ionic conductivity of thick PS-PIL films (50-100 μm) was approximately 20 times higher in the in-plane direction than in the through-plane direction, consistent with a mixed structure comprised of randomly-oriented lamellae throughout the interior of the film and highly-oriented lamellae at the electrode surface. Therefore, to fully optimize the performance of a block copolymer electrolyte, it is important to consider the effects of surface interactions on ordering of domains.

Block copolymers of polymeric ionic liquids (PILs), which consist of a PIL linked to an insulating polymer that provides mechanical stability, are a class of solid polymer electrolytes that show promise in electrochemical energy applications.[1–7] The relationship between self assembled morphology and ionic conductivity in these materials is often quantified by a morphology factor f, defined as

$$f = \sigma_0/(\phi_{\mathrm{PIL}}\sigma_{\mathrm{PIL}}) \tag{1}$$

where σ_0 and σ_{PIL} are the measured DC ionic conductivity of the block copolymer and PIL homopolymer, respectively, and ϕ_{PIL} is the volume fraction of the PIL block in the block copolymer.[8] The theoretical or "ideal" morphology factors for cylindrical, lamellar, and gyroid phases are $f = 1/3$, $2/3$, and 1, respectively.[9] The interpenetrating network of the gyroid phase is desirable for three-dimensional ion transport, but this morphology is difficult to attain due to its narrow window of stability with respect to composition.[10] The lamellar morphology is often investigated because of its stability across a wide composition range as compared to the gyroid phase. Moreover, if some of the ion-conducting lamellae are continuous across grain boundaries, then randomly-oriented lamellar grains can enable long-range ion transport. Morphology factors have been measured for lamellar block copolymer electrolytes using electrochemical impedance spectroscopy in two- or four-point probe configurations, where the electric field is oriented parallel to the plane of the film, and the values are consistent with $f = 2/3$.[8,9,11,12] However, when morphology factors are measured using a parallel plate geometry where the electric field is oriented perpendicular to the plane of the film, the ionic conductivity and corresponding morphology factor are often reduced by

orders of magnitude. This reduction is problematic as many devices (*i.e.*, batteries) require through-film ion transport.

Several studies of block copolymer electrolytes have shown that anisotropy in the ionic conductivity (and morphology factor) is correlated with anisotropy in the self-assembled structure.[13–18] Specifically, the ionic conductivity is enhanced or suppressed when the lamellar domains are oriented parallel or perpendicular to the electric field, respectively (Figure 1a-b). Many studies have sought to enhance ionic conductivity by controlling the lamellar domains orientations through processing techniques that include electric field alignment,[15] shear alignment,[15] magnetic field alignment,[16,17] and topographic templates.[18] However, other studies have shown that a small fraction of the lamellar domains will orient parallel to the plane of the film during thermal[15] or solution[14,15] processing, even though these techniques lack a strong structure-directing field. This spontaneous lamellar alignment might be controlled by a thermodynamic process, such as surface-induced ordering that is driven by selective adsorption of one block at a surface.[19] In fact, in a recent study of gyroid-forming block copolymer electrolytes, the authors proposed that preferential adsorption of an insulating block at an electrode surface was responsible for a reduction of through-film ionic conductivity after thermal annealing.[20]

The role of surface interactions on block copolymer ordering is well documented in the literature, although these effects have not been considered in the design of block copolymer electrolytes. In general, one block is preferred over the other at a surface, and this preferential wetting can drive layering of domains through the thickness of a thin film (ca. 100 nm - 1 μm).[21–23] If such a phenomenon occurs in lamellar PIL-containing block copolymer electrolytes, then the highly-oriented layers at an electrode would produce an anisotropic ionic conductivity. This point is illustrated using a simple model for ionic conductivity based on an effective medium approximation.[24] The oriented lamellar structure can be approximated as a series of parallel layers of alternating conducting and insulating domains. If the electric field is aligned parallel to the layers (in-plane conductivity, $\sigma^{\parallel}_{\text{eff}}$), then the effective conduc-

tivity of the material can be estimated from the arithmetic mean of the conductivities of the two blocks (Figure 1a).[25] However, if the conductivity is measured with the electric field perpendicular to the layers (through-plane conductivity, $\sigma^{\perp}_{\text{eff}}$), then the effective conductivity is best approximated by the geometric mean of the conductivities of the two blocks because the insulating domain will dominate (Figure 1b).[25]

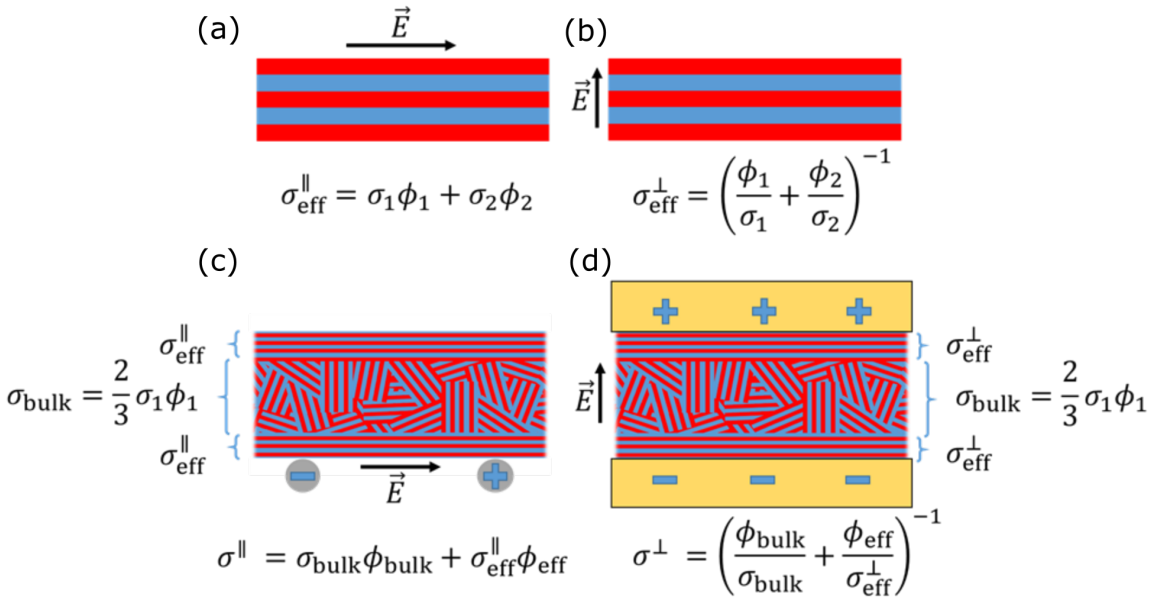

Figure 1: A simple effective medium approximation is used to examine ionic conductivity as a function of lamellar orientation relative to the direction of the applied electric field. For alternating layers of material 1 and material 2, the effective conductivity is described by an arithmetic mean (a) or geometric mean (b) depending on the relative orientation of the electric field. Extending the same method to films that have layering at the interfaces and a polygrain bulk structure (c,d) gives rise to significant anisotropy in the conductivity.

Block copolymer electrolytes are usually processed into thick films (ca. 10 to 100 μm), and the influence of surface interactions on ordering will decay with distance into the film. For lamellar block copolymers, this means that two distinct structures are anticipated: highly-oriented lamellae at the interfaces and randomly-oriented lamellae in the bulk. The effective conductivity of this morphology can be estimated by the same simple methods described in Figure 1a-b, treating the highly-oriented lamellae at the interface as one distinct component and the randomly-oriented lamellae in the bulk as another. The conductivity of the interfacial

regions in the in-plane and through-plane directions is then ${\sigma^{\parallel}}_{\text{eff}}$ and ${\sigma^{\perp}}_{\text{eff}}$, respectively, where the bulk conductivity is estimated by assuming a theoretical morphology factor of $f = 2/3$ for the randomly-oriented lamellae. This simple analysis predicts a highly anisotropic conductivity, with the in-plane value of $\sigma^{\parallel}$ being orders of magnitude higher than the through-plane value of $\sigma^{\perp}$ (Figure 1c-d). Examples of these predictions are included in the Supporting Information Figure S2.

The objective of this study is to demonstrate that PIL-containing block copolymers will form highly-oriented layers at the interface with the electrode, a consequence of preferential wetting by one block at the electrode surface, leading to significant anisotropy in the ionic conductivity. The materials investigated are two lamellar diblock copolymers of polystyrene (PS) and poly(1-(2-acryloyloxyethyl)-3-butylimidazolium bis(trifluoromethanesulfonyl)imide) (PIL) having different molecular weights, as well as a PIL homopolymer for comparison (Table 1). All materials were synthesized via reversible addition-fragmentation chain transfer (RAFT) polymerization. Molecular weight dispersities were determined by gel permeation chromatography (GPC) against polystyrene standards, and were less than 1.3 for all samples. The molecular weights of the PS blocks were determined by GPC and confirmed by nuclear magnetic resonance spectroscopy (NMR) using end group analysis. The molecular weights of PIL blocks were determined as described in the Supporting Information. The volume fractions of PIL in the PS-PIL block copolymers, ϕ_{PIL}, were calculated from the molecular weights of each block using a density of of 1.04 g/mL for PS and 1.38 g/mL for PIL.[11]

The bulk self-assembled structure of the block copolymer samples was examined using transmission small-angle x-ray scattering (SAXS). Samples were annealed at 120 °C for 24 hours. The azimuthally-integrated intensity for both block copolymer samples are shown in Figure 2a. Sample PS6-PIL47 shows peaks at a $q^{\star}$:$2q^{\star}$:$3q^{\star}$ ratio, where $q^{\star} = 0.036$ Å^{-1}, indicative of lamellae with a domain periodicity of d_0=17.5 nm. The intensity of the $2q^{\star}$ peak is reduced relative to the $q^{\star}$ and $3q^{\star}$ peaks, which is expected as this position coincides

Table 1: Characteristics of Polymers and Copolymers.

Sample Name	$M_{n,PS}$[a] (g/mol)	$M_{n,PIL}$[b] (g/mol)	ϕ_{PIL}[b]	Đ[c]	$T_{g,PS}$[d] (°C)	$T_{g,PIL}$[d] (°C)
PS	10,000	–	0.0	1.17	91.4	–
PIL	–	14,900	1.0	1.27	–	-10.4
PS4-PIL53	4000	6500	0.53	1.28	72.0	0.0
PS6-PIL47	6000	7600	0.47	1.29	84.9	-3.7

[a]Determined by GPC and NMR; [b]determined by NMR; [c]determined by GPC of the homopolymer or block copolymer prior to quaternization; [d]determined by differential scanning calorimetry (DSC).

with a minimum in the form factor of equal-volume lamellae. PS4-PIL53 shows a single sharp peak at $q^\star$, which indicates a high degree of order, but the higher-order peaks are not observed. It can be reasonably inferred from the PIL volume fraction that the sample organizes into a lamellar structure with a domain periodicity of $d_0 = 10.8$ nm; the absence of the $2q^\star$ peak is attributable to a minimum in the form factor, while the absence of the $3q^\star$ peak is attributable to interface attenuation resulting from a weaker segregation strength due to lower molecular weight.[26,27] The 2D scattering data (see Figures S9-S10 in the Supporting Information) for both copolymer films show no indication of anisotropy, demonstrating that the bulk structure adopted by both samples is randomly-oriented lamellae. The full width at half maximum (fwhm) of the $q^\star$ peak is 0.0029 $Å^{-1}$ and 0.0027 $Å^{-1}$ for PS6-PIL47 and PS4-PIL53, respectively. Using the Scherrer equation,[28] the bulk grain size ($\approx 2\pi$/fwhm) is approximately 0.2 μm in both materials.

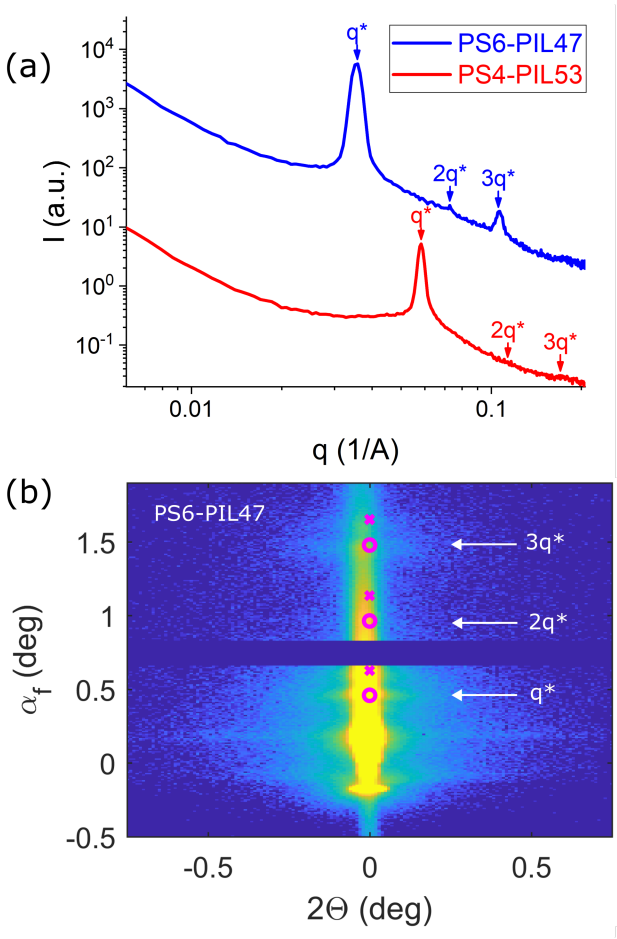

Figure 2: (a) Azimuthally-integrated SAXS data of bulk block copolymer samples. (b) GISAXS data of PS6-PIL47 thin film (300 nm) flow coated on silicon, measured at an incidence angle of 0.18°.

The effect of surfaces on lamellar self-assembly was probed through grazing-incidence small-angle x-ray scattering (GISAXS), microscopy and contact angle goniometry from thin films annealed at 120 °C for 24 hours. Representative GISAXS data for a 300 nm film of PS6-PIL47 on silicon are shown in Figure 2b as a function of in-plane (2θ) and out-of-plane (α_f) scattering angles. The scattering was concentrated into Bragg peaks along the out-of-plane direction, which is a signature of lamellar layers through the film thickness. The positions of the two Bragg peaks for each order of reflection (q*, 2q*, 3q*) were predicted for a lamellar periodicity of 17 nm and incidence angle of 0.18°, following procedures described elsewhere,[29] and are marked by the "x" and "o" symbols in Figure 2b. The predicted Bragg

peak positions for $q^\star$ and $3q^\star$ agree with the experimental data. As with the SAXS data, the peaks associated with the even reflection ($2q^\star$) are not observed.

Another signature of surface-induced layering of lamellar domains in thin films is island and hole formation, which arises when the thickness of the as-cast film is incommensurate with the thickness of each lamellar domain.[23] When both the air surface and substrate are preferential to one block, the height of islands (and depth of holes) is equal to d_0. Films of PS4-PIL53 and PS6-PIL47 having thickness gradients were prepared by flow coating from either THF or acetonitrile. The as-cast films showed a continuous transition in thickness along the flow coating direction. However, after thermal annealing, the films separated into regions of discrete thicknesses that were separated by islands and holes. Optical microscopy data for PS6-PIL47 in Figure 3a shows the islands and holes between these regions of discrete thicknesses. Atomic force microscopy data for the same sample in Figures 3b-c demonstrates that the height of islands is equal to approximately 17 nm, consistent with measurements of d_0 obtained from bulk SAXS and thin film GISAXS measurements.

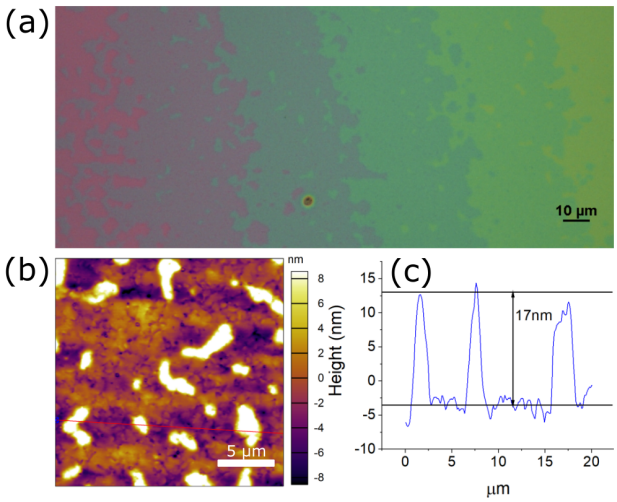

Figure 3: Island and hole formation observed in thin film of PS6-PIL47 is observed by optical microscopy (a) and AFM (b). The film was annealed at 120 °C for 24 h. The AFM tapping mode height image is 20×20 μm^2. Cross-section of the AFM height image (c) shows island height is approximately equal to $d_0 = 17$ nm.

To identify the block that is present at the air surface, water contact angles were recorded

from thin films of each block copolymer, as well as from PS and PIL homopolymers. These data are reported in Table 2. The average water contact angle for both block copolymer films and for the PIL homopolymer was in the range of 74 to 77°, while the average water contact angle on PS homopolymer was 91°. While no direct measurement could be made of the wetting behavior at the silicon substrate, the more polar PIL block is likely preferred over PS on the thin native oxide at this boundary. The interfacial structure that results from preferential wetting at an air surface and silicon substrate is relevant to measurements of the in-plane (Figure 1c) and through-plane (Figure 1d) ionic conductivity, respectively.

Table 2: Static water contact angles on thin films flow-coated on silicon. The average water contact angle is calculated from three measurements per sample, and the uncertainty is reported as ±1 standard deviation.

Sample Name	θ (°)
PS	91.1 ± 0.4
PIL	74.0 ± 1.3
PS4-PIL53	74.8 ± 1.8
PS6-PIL47	76.8 ± 1.5

The SAXS measurements of bulk PS-PIL samples reveal randomly-oriented lamellae, while thin film experiments reveal layers of lamellae between the air surface and silicon substrate. It is reasonable to expect that a thick film of PS-PIL will have randomly-oriented lamellae throughout most of the thickness, with highly-oriented lamellar layers at each surface. This statement is supported by GISAXS measurements of a thick film on a silicon substrate (ca. 100 μm), which show a mixture of highly-oriented and randomly-oriented lamellar domains (see Supporting Information Figure S11). However, the films are thick and the free surfaces are rough due to the solution-casting process. As a result, GISAXS cannot quantify the depth-dependent distribution of domain orientations.

The ionic conductivity of these materials was measured using impedance spectroscopy with two different electrode configurations. The in-plane ionic conductivity of both PS-PIL block copolymer and PIL homopolymer samples was measured using a two-point probe configuration, as illustrated in Figure 1c. The through-plane conductivity was measured

using a parallel plate configuration, which means the films are sandwiched between two electrodes. Two types of electrodes were used for through-plane measurements, highly-doped silicon and brass, and both yielded the same results. All films were 40-100 μm thick and annealed at 120 °C for 24 hours prior to impedance spectroscopy measurements at room temperature (20 °C). Procedures for sample preparation and measurement using the two-point and parallel plate configurations are detailed in the Supporting Information. The results of the impedance measurements of both electrode geometries are summarized in Table 3. The measured ionic conductivity of the PIL homopolymer was similar along the in-plane and through-plane directions. For both block copolymer samples, however, the in-plane ionic conductivity was approximately 20 times greater than the through-plane ionic conductivity.

Table 3: Summary of conductivity data (S/cm) at 20 °C.

Sample Name	${\sigma_{dc}}^{\parallel a}$(S/cm)	${\sigma_{dc}}^{\perp b}$(S/cm)	$f^{\parallel c}$	$f^{\perp c}$	a^d
PIL	1.0×10^{-6}	7.7×10^{-7}	–	–	1.3
PS4-PIL53	1.8×10^{-7}	8.1×10^{-9}	0.32	0.033	22
PS6-PIL47	3.0×10^{-7}	1.2×10^{-8}	0.62	0.024	26

[a]In-plane DC conductivity, determined by impedance spectroscopy in two-point electrode configuration; [b]through-plane DC conductivity, determined by impedance spectroscopy in parallel plate electrode configuration; [c]morphology factors calculated via Equation 1; [d]ratio of ${\sigma_{dc}}^{\parallel}$ to ${\sigma_{dc}}^{\perp}$.

The morphology factors calculated from the in-plane ionic conductivities are consistent with those reported for similar materials that were also characterized by in-plane impedance spectroscopy measurements.[11,12] PS6-PIL47 exhibited a morphology factor of 0.62, in good agreement with the theoretical value of 2/3 for randomly oriented lamellae. Sample PS4-PIL53 exhibited a lower morphology factor of 0.3, possibly resulting from broader interfacial regions between domains due to reduced segregation strength. In contrast, the morphology factors calculated from the through-plane data decrease by more than an order of magnitude compared to their in-plane counterparts. This discrepancy between in-plane and through-plane conductivity is consistent with highly-oriented lamellar layers at the interface with the electrodes. Both in-plane and through-plane measurements of ionic conductivity are probing

two distinct structures within the film: an interfacial region of highly-oriented lamellae and a bulk region of randomly-oriented lamellae. Both structures contribute to ion transport in the in-plane direction, whereas ion transport in the through-plane direction is impeded by the presence of insulating PS layers at the interfaces.

In summary, these studies demonstrate that preferential interactions at an electrode or air surface will drive alignment of lamellar PS-PIL domains parallel to the plane of a film. As a result, the structure of PS-PIL thick films is comprised of randomly-oriented lamellae in the bulk and highly-oriented lamellae at surfaces. A consequence of the two distinct structures is a corresponding anisotropy in the DC ionic conductivity, with in-plane ionic conductivity exhibiting a more than twenty-fold increase over the through-plane ionic conductivity, an outcome that is consistent with simple models based on an effective medium approximation. Anisotropy in the DC ionic conductivity has significant implications with respect to applications such as lithium ion batteries, as ion transport is generally required in the through-plane direction. It is important to note that surface-induced ordering is likely encountered with other types of block copolymer electrolytes, as there are few examples of chemically-distinct polymers that are equally attracted to the same boundary.[19] However, one could suppress preferential interactions at a surface using methods that are already established for block copolymer lithography, including surface-active additives or thin "neutral" coatings on the electrodes.[30,31]

Acknowledgement

J.P.C. and G.E.S. acknowledge financial support from the National Science Foundation under Award No. DMR-1731292. J.P.C., G.E.S., and S.M.K.II acknowledge financial support from the National Science Foundation under Award No. DMR-1905487. J.S. acknowledges support by the National Science Foundation, the Division of Chemistry through Award No. CHE-1753282. T.K. gratefully acknowledges financial support from the U.S. Army Re-

search Office under Contract No. W911NF-17-1-0052. GISAXS measurements were enabled by the Major Research Instrumentation program of the National Science Foundation under Award No. DMR-1827474. GISAXS and DSC measurements were performed at the University of Tennessee Polymer Characterization Laboratory. Transmission SAXS measurements were performed through the South Carolina SAXS Collaborative at the University of South Carolina. The authors thank Elizabeth O'Connell for assistance with NMR analysis.

Supporting Information Available

Discussion of effective medium approximation model of conductivity in BCP films with oriented lamellae at the interfaces; summary of monomer and polymer synthesis and characterization of polymer properties; summary of film casting and characterization; supplemental scattering data; conductivity measurement procedures.

References

(1) Nykaza, J. R.; Benjamin, R.; Meek, K. M.; Elabd, Y. A. Polymerized ionic liquid diblock copolymer as an ionomer and anion exchange membrane for alkaline fuel cells. *Chemical Engineering Science* **2016**, *154*, 119–127, DOI: 10.1016/j.ces.2016.05.041.

(2) Nykaza, J. R.; Savage, A. M.; Pan, Q.; Wang, S.; Beyer, F. L.; Tang, M. H.; Li, C. Y.; Elabd, Y. A. Polymerized ionic liquid diblock copolymer as solid-state electrolyte and separator in lithium-ion battery. *Polymer* **2016**, *101*, 311–318, DOI: 10.1016/j.polymer.2016.08.100.

(3) Morris, M. A.; An, H.; Lutkenhaus, J. L.; Epps, T. H. Harnessing the power of plastics: Nanostructured polymer systems in lithium-ion batteries. *ACS Energy Letters* **2017**, *2*, 1919–1936, DOI: 10.1021/acsenergylett.7b00368.

(4) Ketkar, P. M.; Shen, K. H.; Hall, L. M.; Epps, T. H. Charging toward improved lithium-ion polymer electrolytes: Exploiting synergistic experimental and computational approaches to facilitate materials design. *Molecular Systems Design and Engineering* **2019**, *4*, 223–238, DOI: 10.1039/c8me00105g.

(5) Young, W. S.; Kuan, W. F.; Epps, T. H. Block copolymer electrolytes for rechargeable lithium batteries. *Journal of Polymer Science, Part B: Polymer Physics* **2014**, *52*, 1–16, DOI: 10.1002/polb.23404.

(6) Sanoja, G. E.; Popere, B. C.; Beckingham, B. S.; Evans, C. M.; Lynd, N. A.; Segalman, R. A. Structure-Conductivity Relationships of Block Copolymer Membranes Based on Hydrated Protic Polymerized Ionic Liquids: Effect of Domain Spacing. *Macromolecules* **2016**, *49*, 2216–2223, DOI: 10.1021/acs.macromol.5b02614.

(7) Evans, C. M.; Sanoja, G. E.; Popere, B. C.; Segalman, R. A. Anhydrous Proton Transport in Polymerized Ionic Liquid Block Copolymers: Roles of Block Length, Ionic Content, and Confinement. *Macromolecules* **2016**, *49*, 395–404, DOI: 10.1021/acs.macromol.5b02202.

(8) Wanakule, N. S.; Panday, A.; Mullin, S. A.; Gann, E.; Hexemer, A.; Balsara, N. P. Ionic conductivity of block copolymer electrolytes in the vicinity of order-disorder and order-order transitions. *Macromolecules* **2009**, *42*, 5642–5651, DOI: 10.1021/ma900401a.

(9) Hallinan Jr., D. T.; Balsara, N. P. Polymer electrolytes. *Annu. Rev. Mater. Res.* **2013**, *43*, 503–525, DOI: 10.1146/annurev-matsci-071312-121705.

(10) Cochran, E. W.; Garcia-Cervera, C. J.; Fredrickson, G. H. Stability of the gyroid phase in diblock copolymers at strong segregation. *Macromolecules* **2006**, *39*, 2449–2451, DOI: 10.1021/ma0527707.

(11) Choi, J. H.; Ye, Y.; Elabd, Y. A.; Winey, K. I. Network structure and strong mi-

crophase separation for high ion conductivity in polymerized ionic liquid block copolymers. *Macromolecules* **2013**, *46*, 5290–5300, DOI: 10.1021/ma400562a.

(12) Weber, R. L.; Ye, Y.; Schmitt, A. L.; Banik, S. M.; Elabd, Y. A.; Mahanthappa, M. K. Effect of nanoscale morphology on the conductivity of polymerized ionic liquid block copolymers. *Macromolecules* **2011**, DOI: 10.1021/ma201067h.

(13) Cheng, S.; Smith, D. M.; Pan, Q.; Wang, S.; Li, C. Y. Anisotropic ion transport in nanostructured solid polymer electrolytes. *RSC Advances* **2015**, *5*, 48793–48810, DOI: 10.1039/c5ra05240h.

(14) Gwee, L.; Choi, J. H.; Winey, K. I.; Elabd, Y. A. Block copolymer/ionic liquid films: The effect of ionic liquid composition on morphology and ion conduction. *Polymer* **2010**, *51*, 5516–5524, DOI: 10.1016/j.polymer.2010.09.026.

(15) Park, M. J.; Balsara, N. P. Anisotropic proton conduction in aligned block copolymer electrolyte membranes at equilibrium with humid air. *Macromolecules* **2010**, *43*, 292–298, DOI: 10.1021/ma901980b.

(16) Majewski, P. W.; Gopinadhan, M.; Jang, W.-S.; Lutkenhaus, J. L.; Osuji, C. O. Anisotropic Ionic Conductivity in Block Copolymer Membranes by Magnetic Field Alignment. *J. Am. Chem. Soc.* **2010**, *132*, 17516–17522, DOI: 10.1021/ja107309p.

(17) Majewski, P. W.; Gopinadhan, M.; Osuji, C. O. The effects of magnetic field alignment on lithium ion transport in a polymer electrolyte membrane with lamellar morphology. *Polymers* **2019**, *11*, DOI: 10.3390/polym11050887.

(18) Kambe, Y.; Arges, C. G.; Czaplewski, D. A.; Dolejsi, M.; Krishnan, S.; Stoykovich, M. P.; De Pablo, J. J.; Nealey, P. F. Role of Defects in Ion Transport in Block Copolymer Electrolytes. *Nano Letters* **2019**, *19*, 4684–4691, DOI: 10.1021/acs.nanolett.9b01758.

(19) Stein, G. E.; Laws, T. S.; Verduzco, R. Tailoring the Attraction of Polymers toward Surfaces. *Macromolecules* **2019**, *52*, 4787–4802, DOI: 10.1021/acs.macromol.9b00492.

(20) Sutton, P.; Bennington, P.; Patel, S. N.; Stefik, M.; Wiesner, U. B.; Nealey, P. F.; Steiner, U.; Gunkel, I. Surface Reconstruction Limited Conductivity in Block-Copolymer Li Battery Electrolytes. *Advanced Functional Materials* **2019**, *29*, 1–9, DOI: 10.1002/adfm.201905977.

(21) Albert, J. N.; Epps, T. H. Self-assembly of block copolymer thin films. *Materials Today* **2010**, *13*, 24–33, DOI: 10.1016/S1369-7021(10)70106-1.

(22) Segalman, R. A. Patterning with block copolymer thin films. *Mater. Sci. Eng. R* **2005**, *48*, 191–226, DOI: 10.1016/j.mser.2004.12.003.

(23) Fasolka, M. J.; Mayes, A. M. Block Copolymer Thin Films: Physics and Applications. *Annu. Rev. Mater. Res.* **2001**, *31*, 323–355, DOI: 10.1146/annurev.matsci.31.1.323.

(24) Sax, J.; Ottino, J. M. Modeling of transport of small molecules in polymer blends: Application of effective medium theory. *Polymer Engineering and Science* **1983**, *23*, 165–176, DOI: 10.1002/pen.760230310.

(25) Torquato, S. *Random Heterogeneous Materials*; Springer Science+Business Media, 2002.

(26) Stein, G. E.; Liddle, J. A.; Aquila, A. L.; Gullikson, E. M. Measuring the Structure of Epitaxially Assembled Block Copolymer Domains with Soft X-ray Diffraction. *Macromolecules* **2010**, *43*, 433–441, DOI: 10.1021/ma901914b, WOS:000273268700057.

(27) Burns, A. B.; Christie, D.; Mulhearn, W. D.; Register, R. A. Estimating the segregation strength of microphase-separated diblock copolymers from the interfacial width. *Journal of Polymer Science Part B: Polymer Physics* **2019**, *57*, 932–940, DOI: 10.1002/polb.24848, https://onlinelibrary.wiley.com/doi/pdf/10.1002/polb.24848.

(28) Guinier, A. *X-Ray Diffraction: In Crystals, Imperfect Crystals, and Amorphous Bodies*; Dover Publications, Inc., 1994.

(29) Stein, G. E.; Kramer, E. J.; Li, X.; Wang, J. Layering Transitions in Thin Films of Spherical-Domain Block Copolymers. *Macromolecules* **2007**, *40*, 2453–2460, DOI: 10.1021/ma0625509.

(30) Bates, C. M.; Maher, M. J.; Janes, D. W.; Ellison, C. J.; Willson, C. G. Block Copolymer Lithography. *Macromolecules* **2014**, *47*, 2–12, DOI: 10.1021/ma401762n.

(31) Wang, H. S.; Kim, K. H.; Bang, J. Thermal Approaches to Perpendicular Block Copolymer Microdomains in Thin Films: A Review and Appraisal. *Macromol. Rapid Commun.* **2019**, *40*, 1800728, DOI: 10.1002/marc.201800728.

Graphical TOC Entry